

## Bouncing localized structures in a liquid-crystal light-valve experiment

M. G. Clerc,<sup>1</sup> A. Petrossian,<sup>2</sup> and S. Residori<sup>2</sup>

<sup>1</sup>Departamento de Física, Facultad de Ciencias Físicas y Matemáticas, Universidad de Chile, Casilla 487-3, Santiago, Chile

<sup>2</sup>Institut Non-Linéaire de Nice, 1361 Route des Lucioles, 06560 Valbonne, France

(Received 27 October 2003; published 25 January 2005)

Experimental evidence of bouncing localized structures in a nonlinear optical system is reported. Oscillations in the position of the localized states are described by a consistent amplitude equation, which we call the Lifshitz normal form equation, in analogy with phase transitions. Localized structures are shown to arise close to the Lifshitz point, where nonvariational terms drive the dynamics into complex and oscillatory behaviors.

DOI: 10.1103/PhysRevE.71.015205

PACS number(s): 42.70.Df, 05.45.-a, 42.65.Sf, 47.54.+r

During the last years localized structures have been observed in different fields, such as domains in magnetic materials [1], chiral bubbles in liquid crystals [2], current filaments in gas discharge experiments [3], spots in chemical reactions [4], pulses [5], kinks [6] and localized two-dimensional (2D) states [7] in fluid surface waves, oscillons in granular media [8], isolated states in thermal convection [9,10], solitary waves in nonlinear optics [11–13], and cavity solitons in lasers [14]. Localized states are patterns that extend only over a small portion of a spatially extended and homogeneous system [15]. Different mechanisms leading to stable localization have been proposed [16]. Among these, two main classes of localized structures have to be distinguished, namely those localized structures arising as solutions of a quintic Swift-Hohenberg-like equation [16] and those that are stabilized by nonvariational terms in the subcritical Ginzburg-Landau equation [17]. The main difference between the two cases is that the first-type localized structures have a characteristic size that is fixed by the pinning mechanism over the underlying pattern or by spatially damped oscillations between homogeneous states [16,18], whereas the second-type ones have no intrinsic spatial length, their size being selected by nonvariational effects and going to infinity when dissipation goes to zero. In both cases, nonvariational effects may lead to dynamical behaviors of localized structures [19]. Variational models based on a generalized Swift-Hohenberg equation have been proposed to describe the appearance of localized structures in nonlinear optics [20]. However, a generalization, including nonvariational terms, is generically expected to apply even in optics, as happens, for instance, in semiconductor laser instabilities [21], giving rise to dynamical behaviors of localized structures, such as propagation and oscillations of their positions [22].

We report here an experimental evidence of localized structures dynamics in a liquid crystal light valve (LCLV) with optical feedback. It is already known that, in the simultaneous presence of bistability and pattern-forming diffractive feedback, the LCLV system shows localized structures [12,23–25]. Recently, rotation of localized structures along concentric rings have been reported in the case of a rotation angle introduced in the feedback loop [26]. Here, we fix a zero rotation angle and we show a dynamical behavior—the bouncing of two adjacent localized structures—that is not related to imposed boundary conditions but is instead a direct consequence of the nonvariational character of the system

under study. Theoretically, we show that the LCLV system has several branches of bistability connecting a homogeneous state to a patterned one and we derive an amplitude equation accounting for the appearance of localized structures. This is a one-dimensional model, which we call the Lifshitz normal form equation [22], characterizing the dynamics of localized structures close to each point of nascent bistability.

*Description of the experiment.* The experimental setup is shown in Fig. 1. The LCLV is composed of a nematic liquid crystal film sandwiched in between a glass and a photoconductive plate over which a dielectric mirror is deposited. The liquid crystal film is planar aligned (nematic director  $\vec{n}$  parallel to the walls), with a thickness  $d=15\ \mu\text{m}$ . The liquid crystal filling our LCLV is the nematic LC-654, produced by the research center Organic Intermediates and Dye Institut, NIOPIK (Moscow) [27]. It is a mixture of cyano-biphenyls, with a positive dielectric anisotropy  $\Delta\varepsilon=\varepsilon_{\parallel}-\varepsilon_{\perp}=+10.7$  and large optical birefringence,  $\Delta n=n_{\parallel}-n_{\perp}=0.2$ , where  $\varepsilon_{\parallel}$  and  $\varepsilon_{\perp}$  are the dielectric permittivities  $\parallel$  and  $\perp$  to  $\vec{n}$ , respectively, and  $n_{\parallel}$  and  $n_{\perp}$  are the extraordinary ( $\parallel$  to  $\vec{n}$ ) and ordinary ( $\perp$  to  $\vec{n}$ ) refractive index, respectively. Transparent electrodes over the glass plates permit the application of an electrical voltage across the liquid crystal layer. The photoconductor behaves like a variable resistance, which decreases for increasing illumination. The feedback is obtained by sending back onto the photoconductor the light that has passed through the liquid-crystal layer and has been reflected by the dielectric mirror. This light beam experiences a phase shift

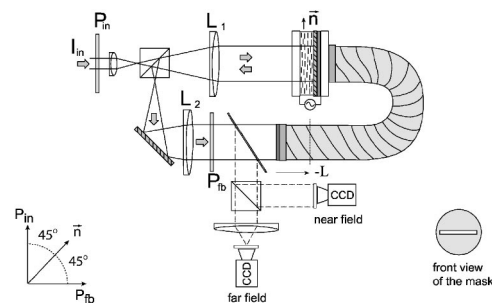


FIG. 1. Experimental setup:  $\vec{n}$  liquid crystal nematic director;  $P_{in}$  and  $P_{fb}$  input and feedback polarizers;  $L_1$  and  $L_2$  confocal 25 cm focal length lenses.  $-L$  is the free propagation length, negative with respect to the plane on which a 1:1 image of the front side of the LCLV is formed.

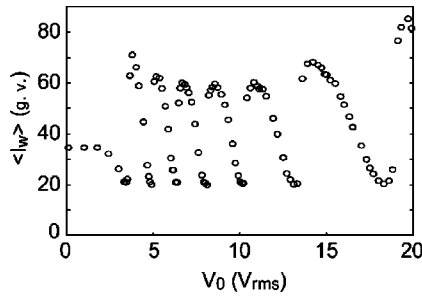


FIG. 2. Spatially averaged feedback intensity  $\langle I_w \rangle$  (units are the gray values, g.v., on the CCD camera) as a function of  $V_0$ ; input intensity  $I_{in}=0.75$  mW/cm<sup>2</sup>.

that depends on the liquid crystal reorientation and, on its turn, modulates the effective voltage that locally applies to the liquid crystals.

The feedback loop is closed by an optical fiber bundle and is designed in such a way that diffraction and polarization interference are simultaneously present [12]. The optical free propagation length is fixed to  $L=-10$  cm. At the linear stage for the pattern formation, a negative propagation distance selects the first unstable branch of the marginal stability curve, as for a focusing medium. The angles of the polarizers are at  $45^\circ$  with respect to the liquid crystal director  $\vec{n}$ . The free end of the fiber bundle is mounted on a precision rotation and translation stage, to avoid rotation or translation in the feedback loop.

For this parameter setting, as  $V_0$  increases there is a series of successive branches of bistability between a periodic pattern and a homogeneous solution. In Fig. 2 we report the spatially averaged feedback intensity  $\langle I_w \rangle$  measured for a fixed value of the input intensity,  $I_{in}=0.75$  mW/cm<sup>2</sup>, and for varying  $V_0$ , by integrating the images on the near-field charge-coupled device (CCD) camera (see Fig. 1). The abrupt changes of  $\langle I_w \rangle$  correspond to the appearance of localized structures and thus roughly indicate the locations of the nascent bistability points. The peak value intensity of the localized structures is approximately twice the average value  $\langle I_w \rangle$ . In the LCLV system, the bistability between homogeneous states results from the subcritical character of the Fréedericksz transition, when the local electric field, which applies to the liquid crystals, depends on the liquid crystal reorientation angle [28,29]. Here, we limit our study to the bistable branch located around  $V_0=13.2$  V<sub>rms</sub> (frequency 5 kHz), however similar observations can be obtained close to any other of the nascent bistability points.

We have carried out one-dimensional experiments, in order to avoid the influence of any optical misalignment (such as small drifts) on the dynamics of localized states. A rectangular mask is introduced in the optical feedback loop, just in contact to the entrance side of the fiber bundle. The width of the aperture is  $D=0.50$  mm, whereas its length is  $l=20$  mm. The size of each localized structures is  $\Lambda \approx 350$   $\mu$ m, so that the transverse aspect ratio  $D/\Lambda \approx 1$  is small enough for the system to be considered as one-dimensional and the longitudinal aspect ratio  $l/\Lambda \approx 60$  is large enough for the system to be considered as a spatially extended one.

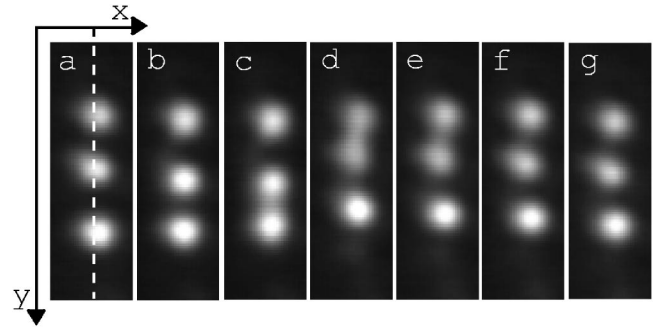


FIG. 3. Snapshots showing bouncing localized structures: (a)  $t=0.0$ , (b) 1.0, (c) 1.3, (d) 1.7, (e) 2.1, (f) 2.4, (g) 2.8 s.

Instantaneous snapshots of bouncing localized structures, together with their spatial profiles, are shown in Figs. 3 and 4, for  $V_0=13.2$  V<sub>rms</sub> and  $I_{in}=0.95$  mW/cm<sup>2</sup>. The corresponding spatiotemporal plot is displayed in Fig. 5(b), showing the periodic oscillations for the positions of the structures. In the same figure, Fig. 5(a), it is shown the spatiotemporal plot corresponding to stationary localized structures, as observed for a slightly decreased input intensity,  $I_{in}=0.90$  mW/cm<sup>2</sup>, and for the same value of  $V_0$ . Figure 5(c) displays the spatiotemporal diagram corresponding to aperiodic oscillations in the structure positions, as observed for  $V_0=13.3$  V<sub>rms</sub> and  $I_{in}=0.90$  mW/cm<sup>2</sup>. The dynamical behavior of localized structures is very sensitive to parameter changes and, even though their appearance is clearly located around each point of nascent bistability, their stability range is smaller than the width of the bistable region. When losing stability, localized structures either form clusters or annihilate, depending if

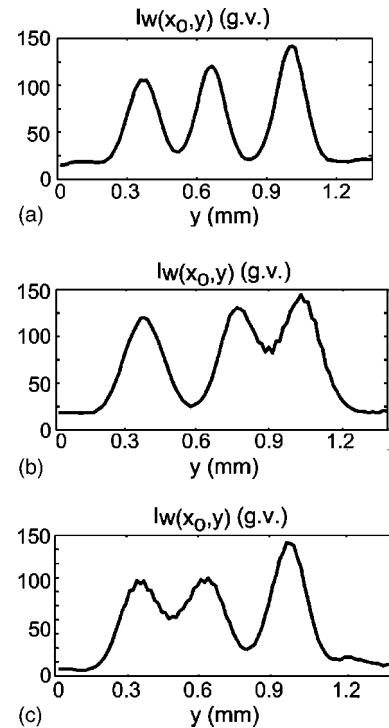


FIG. 4. Localized structures profile,  $I_w(x_0, y)$ .  $x_0$  is the location of the dashed line in Fig. 3; (a)  $t=0.0$ , (b) 1.3, (c) 1.7 s.

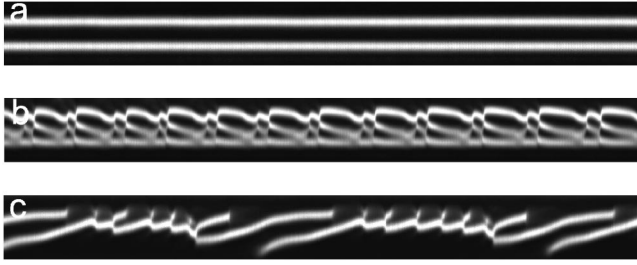


FIG. 5. Space (vertical)-time (horizontal) diagrams showing (a) two stationary localized structures, (b) periodic, and (c) aperiodic oscillations of the structure positions. The total elapsed time is 94 s.

they are driven on the pinning or depinning side of the bistable region [18]. However, a careful experimental characterization of the pinning front is a work still in progress.

*Theoretical description.* The light intensity  $I_w$  reaching the photoconductor is given by [12],  $I_w = I_{in}/2 |e^{-i(L/2k)\partial_{xx}} \times (1 + e^{-i\beta \cos^2 \theta})|^2$ , where  $x$  is the transverse direction of the liquid crystal layer,  $\beta \cos^2 \theta$  is the overall phase shift experienced by the light traveling back and forth through the liquid crystal layer;  $\beta = 2kd\Delta n$ , where  $k = 2\pi/\lambda$  is the optical wave number ( $\lambda = 633$  nm).

As long as  $I_{in}$  is sufficiently small, that is, of the order of a few  $\text{mW}/\text{cm}^2$ , the effective electric field,  $E_{eff}$ , applied to the liquid crystal layer can be expressed as  $E_{eff} = \Gamma V_0/d + \alpha I_w$ , where  $V_0$  is the voltage applied to the LCLV,  $0 < \Gamma < 1$  is a transfer factor that depends on the electrical impedances of the photoconductor, dielectric mirror and liquid crystals, and  $\alpha$  is a phenomenological dimensional parameter that describes the linear response of the photoconductor [29].

Let us call  $\theta(x, t)$  the average director tilt.  $\theta = 0$  is the initial planar alignment whereas  $\theta = \pi/2$  is the homeotropic alignment corresponding to saturation of the molecular reorientation. The dynamics of  $\theta$  is described by a local relaxation equation of the form

$$\tau \partial_t \theta = l^2 \partial_{xx} \theta - \theta + \frac{\pi}{2} \left( 1 - \sqrt{\frac{\Gamma V_{FT}}{\Gamma V_0 + \alpha I_w(\theta, \partial_x)}} \right) \quad (1)$$

with  $V_{eff} = E_{eff}d = \Gamma V_0 + \alpha I_w(\theta, \partial_x) > \Gamma V_{FT}$  the effective voltage applied to the liquid crystals,  $V_{FT}$  the threshold for the Fréedericksz transition and  $l$  the electric coherence length. The above model has been deduced by fitting the experimental data for the open loop response of the LCLV [29] and it is slightly different with respect to the one proposed in Ref. [12]. It is important to note that a rigorous derivation of the response function of the LCLV would require a modal expansion along the longitudinal direction of the liquid crystal layer.

The homogeneous equilibrium solutions are  $\theta_0 = 0$  when  $V_{eff} \leq \Gamma V_{FT}$  and  $\theta_0 = (\pi/2)(1 - \sqrt{\Gamma V_{FT}/V_{eff}})$  when  $V_{eff} > \Gamma V_{FT}$ . Above the Fréedericksz transition and by neglecting the spatial terms, we can find a closed expression for the homogeneous equilibrium solutions:  $\theta_0 = (\pi/2)(1 - \sqrt{\Gamma V_{FT}/[\Gamma V_0 + \alpha I_{in}[1 + \cos(\beta \cos^2 \theta_0)]]})$ . The value of  $V_{FT}$  is set to  $3.2 V_{rms}$ , as measured for the LCLV [28,29], and the graph of  $\theta_0(V_0, I_{in})$  is plotted in Fig. 6. In agreement with the

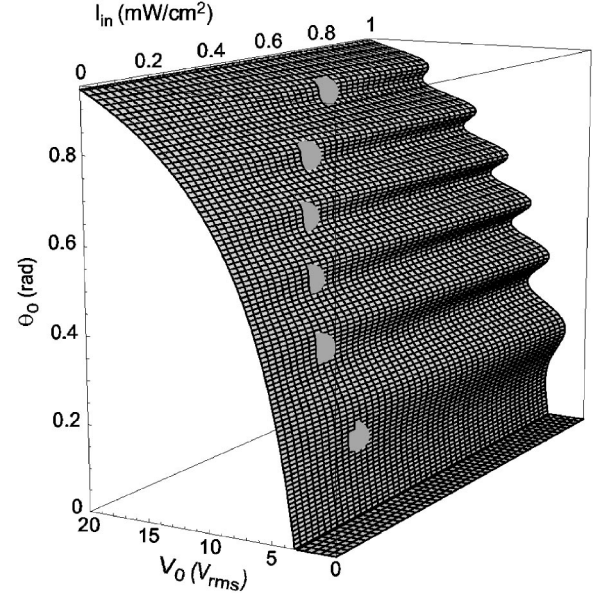


FIG. 6. The multivalued function  $\theta_0(V_0, I_{in})$ . The shaded areas show the location of the nascent bistability points.

bistability branches observed experimentally, several points of nascent bistability can be distinguished, corresponding to the critical points where  $\theta_0(V_0, I_{in})$  becomes a multivalued function.

Close to each point of nascent bistability, and neglecting spatial derivatives, we can develop  $\theta = \theta_0 + u + \dots$  and derive a normal form equation describing an imperfect pitchfork bifurcation [15],  $\partial_t u = \eta + \mu u - u^3 + h.o.t.$ , where  $\mu$  is the bifurcation parameter and  $\eta$  accounts for the asymmetry between the two homogeneous states. Higher-order terms are ruled out by the scaling analysis, since  $u \sim \mu^{1/2}$ ,  $\eta \sim \mu^{3/2}$ , and  $\partial_t \sim \mu$ ,  $\mu \ll 1$ . If we now consider the spatial effects, due to the elasticity of the liquid crystal and to the light diffraction, the system exhibits a spatial instability as a function of the diffraction length and, since the spatial dependence of  $I_w$  is nonlocal, the dynamics is a nonvariational one.

The confluence of bistability and spatial bifurcation give rise to a critical point of codimension three, which we call the Lifshitz point, in analogy with the triple point introduced for phase transitions in helicoidal ferromagnetic states [30]. Close to this point, we derive an amplitude equation, which we call the Lifshitz normal form [22],

$$\partial_t u = \eta + \mu u - u^3 + \nu \partial_{xx} u - \partial_{xxx} u + d u \partial_{xx} u + c (\partial_x u)^2, \quad (2)$$

where  $\partial_x \sim \mu^{1/4}$ ,  $\nu \sim \mu^{1/2}$  accounts for the intrinsic length of the system (diffusion),  $d \sim O(1)$ , and  $c \sim O(1)$ . The term  $\partial_{xxx} u$  describes a super diffusion, accounting for the short distance repulsive interaction, whereas the terms proportional to  $d$  and  $c$  are, respectively, the nonlinear diffusion and convection. The full and lengthy expressions of these coefficients, as a function of the LCLV parameters, will be reported elsewhere [31]. Note that the same model has been recently deduced for instabilities in a semiconductor laser [21].



The model shows bistability between a homogeneous and a spatially periodic solutions and therefore exhibits a family of localized structures. Depending on the choice of parameters, localized structures may show periodic or aperiodic oscillations of their position. We can fix  $\mu$  and  $\eta$  by varying  $V_0$  and  $I_{in}$ . More interesting is the behavior of the effective diffusion term  $\nu$ , which has the form  $\nu \propto l^2 + \{\pi\beta L \cos^2[(\beta/2) \cos^2 \theta_0] \sin 2\theta_0\} / 4k\{\Gamma V_0 + \alpha I_{in}[1 + \cos(\beta \cos^2 \theta_0)]\}$ . Only when the optical free propagation length  $L$  is negative it is possible, by increasing the input intensity  $I_{in}$ , to drive the system through the Lifshitz point ( $\nu$  changes its sign from positive to negative). This means that stable localized structures can be obtained only for a focusing Kerr-like nonlinearity. Once crossed the Lifshitz point, the nonlinear diffusion coefficient is negative and the convection coefficient is positive. In this region of parameters, numerical simulations of Eq. (2) show a qualitative agreement with the experimental observations, as shown in Fig. 7.

**Conclusion.** We have shown a localized structure dynamics, consisting of a bouncing behavior between two adjacent structures, and we have described it by a universal model, the Lifshitz normal form equation. The Lifshitz equation, which reduces to the generalized Swift-Hohenberg equation for  $\eta=d=c=0$ , has already been used to describe the transition from smectic to helicoidal phase in liquid crystals [32] and the pulse dynamics in reaction diffusion systems [33]. When one neglects the cubic and the nonlinear diffusion

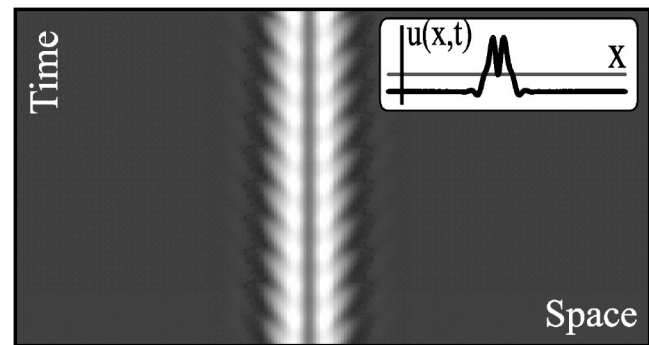


FIG. 7. Numerical simulations of Eq. (2) for  $\eta=-0.02$ ,  $\mu=-0.02$ ,  $\nu=-1.00$ ,  $c=2.00$  and  $d=-1.51$ , showing two bouncing localized structures (spatial profile in the inset).

terms ( $d=0$ ), it reduces to the Nikolaevskii equation that describes longitudinal seismic waves [34].

We gratefully acknowledge René Rojas for help in calculations. The simulation software DIMX is property of INLN. This work has been supported by the ACI Jeunes of the French Ministry of Research (2218 CDR2). M.G.C. thanks the support of Programa de inserción de científicos Chilenos of Fundación Andes, FONDECYT Project No. 1020782, and FONDAP Grant No. 11980002.

- [1] H. A. Eschenfelder, *Magnetic Bubble Technology* (Springer Verlag, Berlin, 1981).
- [2] S. Pirkel, P. Ribiere, and P. Oswald, *Liq. Cryst.* **13**, 413 (1993).
- [3] Y. A. Astrov and Y. A. Logvin, *Phys. Rev. Lett.* **79**, 2983 (1997).
- [4] K-Jin Lee, W. D. McCormick, J. E. Pearson, and H. L. Swinney, *Nature (London)* **369**, 215 (1994).
- [5] J. Wu, R. Keolian, and I. Rudnick, *Phys. Rev. Lett.* **52**, 1421 (1984).
- [6] B. Denardo, W. Wright, S. Putterman, and A. Larraza, *Phys. Rev. Lett.* **64**, 1518 (1990).
- [7] W. S. Edwards and S. Fauve, *J. Fluid Mech.* **278**, 123 (1994).
- [8] P. B. Umbanhowar, F. Melo, and H. L. Swinney, *Nature (London)* **382**, 793 (1996).
- [9] R. Heinrichs, G. Ahlers, and D. S. Cannell, *Phys. Rev. A* **35**, R2761 (1987).
- [10] P. Kolodner, D. Bensimon, and C. M. Surko, *Phys. Rev. Lett.* **60**, 1723 (1988).
- [11] D. W. McLaughlin, J. V. Moloney, and A. C. Newell, *Phys. Rev. Lett.* **51**, 75 (1983).
- [12] R. Neubecker, G. L. Oppo, B. Thuring, and T. Tschudi, *Phys. Rev. A* **52**, 791 (1995).
- [13] B. Schäpers, M. Feldmann, T. Ackemann, and W. Lange, *Phys. Rev. Lett.* **85**, 748 (2000).
- [14] S. Barland *et al.*, *Nature (London)* **419**, 699 (2002).
- [15] M. Cross and P. Hohenberg, *Rev. Mod. Phys.* **65**, 851 (1993).
- [16] P. Coulet, *Int. J. Bifurcation Chaos Appl. Sci. Eng.* **12**, 245 (2002).
- [17] S. Fauve and O. Thual, *Phys. Rev. Lett.* **64**, 282 (1990).
- [18] P. Coulet, C. Riera, and C. Tresser, *Phys. Rev. Lett.* **84**, 3069 (2000).
- [19] See O. Descalzi, Y. Hayase, and H. R. Brand, *Phys. Rev. E* **69**, 026121 (2004) and references therein.
- [20] M. Tlidi, P. Mandel, and R. Lefever, *Phys. Rev. Lett.* **73**, 640 (1994).
- [21] G. Kozyreff, S. J. Chapman, and M. Tlidi, *Phys. Rev. E* **68**, 015201(R) (2002); G. Kozyreff and M. Tlidi, *ibid.* **69**, 066202 (2004).
- [22] M. G. Clerc, *Phys. Lett. A* (to be published).
- [23] P. L. Ramazza, S. Ducci, S. Boccaletti, and F. T. Arecchi, *J. Opt. B: Quantum Semiclassical Opt.* **2**, 399 (2000).
- [24] Y. Iino and P. Davis, *J. Appl. Phys.* **87**, 8251 (2000).
- [25] P. L. Ramazza *et al.*, *Phys. Rev. E* **65**, 066204 (2002).
- [26] S. Residori, T. Nagaya, and A. Petrossian, *Europhys. Lett.* **63**, 531 (2003).
- [27] Further details can be found on the Web site of the manufacturer: <http://www.niopik.ru>
- [28] M. G. Clerc, S. Residori, and C. S. Riera, *Phys. Rev. E* **63**, 060701(R) (2001).
- [29] M. G. Clerc, T. Nagaya, A. Petrossian, S. Residori, and C. S. Riera, *Eur. Phys. J. D* **28**, 435 (2004).
- [30] R. M. Hornreich and M. Luban, *Phys. Rev. Lett.* **35**, 1678 (1975).
- [31] M. G. Clerc, R. Rojas, A. Petrossian, and S. Residori (unpublished).
- [32] A. Michelson, *Phys. Rev. Lett.* **39**, 464 (1977).
- [33] R. Kobayashi, T. Ohta, and Y. Hayase, *Phys. Rev. E* **50**, R3291 (1994).
- [34] M. I. Tribelsky and K. Tsuboi, *Phys. Rev. Lett.* **76**, 1631 (1996).